©2001 The Visualization Society of Japan and Ohmsha, Ltd.
Journal of Visualization, Vol. 4, No. 1 (2001) 73-79

# Flowfield Features on Hypersonic Flow over Rectangular Obstacles

Li, S.-X.*, Chen, Y.-K.* and Ni, Z.-Y.*

* Beijing Institute of Aerodynamics, P.O. Box 7215, Beijing 100074, China.

Received 15 November 2000.
Revised 10 December 2000.

***Abstract*:** The complex separated flows induced by shock wave/boundary layer interaction were studied at hypersonic speed of Mach number 5. The experimental results on hypersonic flow over a set of rectangular cylinders are presented in this paper. The rectangular cylinder mounted on a flat plate worked as a typical model to simulate the obstacle on the vehicle surface. The effects of flow interaction on the aerodynamic characteristics have to be predicted for various geometrical parameters. So the static pressure distributions on the model surface were measured, the complex shock wave system was shown by schlieren photos, and the separated flow patterns around the obstacle were visualized by oil flow technique. All of the results describe the interactive flowfield features including peak pressure levels and their locations as well as separated boundaries associated with influence regions.

***Keywords*:** separated flow, shock wave/boundary layer interaction, flow visualization, hypersonic flow.

## 1. Introduction

During the last five decades, extensive works have been done on the separated flow induced by the shock wave/boundary layer interactions in transonic, supersonic and hypersonic flows. Many works for the two-dimensional flowfield have been obtained for both laminar and turbulent boundary layers. The more complicated three-dimensional flowfields resulting from separation forced by simple protuberances have been reported in some detailed studies and reviewed by Korkegi (1972), Holden (1972), Sedney (1973), Settles and Dolling (1986). The obstacles mounted on the vehicle surface are unavoidable. The induced three-dimensional separation phenomenon is of importance in determining not only the aerodynamic loads but also the aerodynamic heating in these interactive regions. Many different types of shock wave interactions have been observed for various different flow models postulated.

Some are dominated by inviscid effects, whereas viscosity is of prime importance in others. One type of models was chosen as a cylinder with different height scale mounted on the flat plate, such as the contributions by Miller (1966), Dolling and Bogdonoff (1981), Dollong and Smith (1989), Li, et al. (1995)(1996)(2000). In the present paper, a set of rectangular cylinders is used as the test model, which is mounted on a flat plate and the cylinder length scale can be changed from zero to definite height during one test run. The rectangular cylinder with a infinite leading edge radius would induce the largest influence range compared to the definite leading edge radius such as circular cylinder or others. The influence region forced by any definite radius cylinder cannot be beyond that limit range at the same test conditions and height/width scales.

This experimental work was conducted in the hypersonic blowdown wind tunnel with Mach number 5.0 in Beijing Institute of Aerodynamics. The test results are presented in this paper, including measured pressure distributions on the model surface, schlieren photographs and the oil flow patterns to visualize the complex three-dimension separation phenomena based on these measurements. The effects of parameter *H*/*D* (the ratio of height to width of cylinder) on the interactive flowfield are examined.

# 2. Experimental Program

## *2.1 Wind Tunnel and Test Conditions*

The experiments were carried out in the hypersonic blowdown wind tunnel with test section of 17 cm×17 cm. This facility can operate at a nominal freestream Mach number of 5 to 8. For this experiment the Mach number 5.0 and the Reynolds number per meter of $5.3\times10^{7}m^{-1}$ based on freestream flow conditions were chosen. The stagnation pressure of $3\times10^{6}N/m^{2}$ and stagnation temperature of 400K were chosen to ensure the turbulent boundary layer of interest in the measurements. The schlieren photo system was used during the test processing.

The test section was covered by a big tank, and the test model was set up as Fig. 1.

The axis OX is chosen as the center line of the flat plate in freestream flow direction and axis OZ is perpendicular to OX and along the leading edge of the cylinder.

The model geometry and coordinate system are shown in Fig. 1.

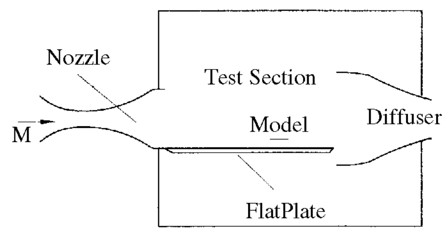


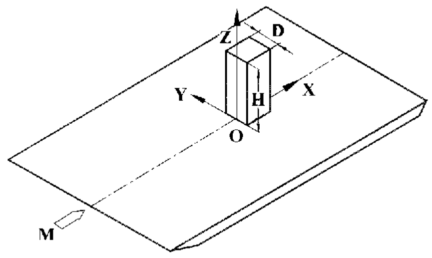


Fig. 1. Model set up and coordinate system.

## *2.2 Model Geometry*

The model consisted of a flat plate and a rectangular cylinder. The flat plate was set up parallel to the freestream direction, and it expanded from the nozzle exit bottom floor. The cylinder was mounted on the flat plate perpendicularly. The distance between the leading edge of the plate and the cylinder was 16.75 cm.

The rectangular cylinder was considered as a circular cylinder with a infinite leading edge radius and two sharp shoulders.

The geometrical characteristics of the model are as following:

The area of the flat plate: $33 \times 24$ cm$^2$

The length of the cylinder $H$: 0~5.5 cm

The width of the cylinder $D$: 2.5 cm

More than 200 holes were made on the flat plate and the cylinder for static pressure measurements. The length of cylinder can be changed from 0 to 5.5 cm during one test run.

## *2.3 Boundary Layer Characteristics*

A fully developed turbulent boundary layer on the flat plate without cylinder was measured. At O point the boundary layer thickness was about 2.2 cm because the boundary layer was developed from channel and nozzle.

During test, the height $H$ of the cylinder was increased from 0 to 5.5 cm, and the shock wave around the leading edge of the cylinder and strong shock wave/turbulent boundary layer interactive phenomena were resulted. The separated flow around the cylinder in a limited region can be visualized by schlieren photos and oil flow patterns. Pressure distributions were measured by pressure transducers.

# 3. Results and Discussions

## *3.1 Flowfield Features*

In present report, a set of shock wave/boundary layer interactive flows is shown by visualization. The boundary layer thickness was of the same order as width of the cylinder. Figure 2 shows a typical flowfield including shock wave system, separated boundary and the reattached line on the flat plate and the cylinder (the skin friction lines converged to the separation line and diverged from the reattached line). The separated region is also marked in the figure. The bow shock was dominated by 2D inviscid flow. However somewhere below triple point the viscosity became important.

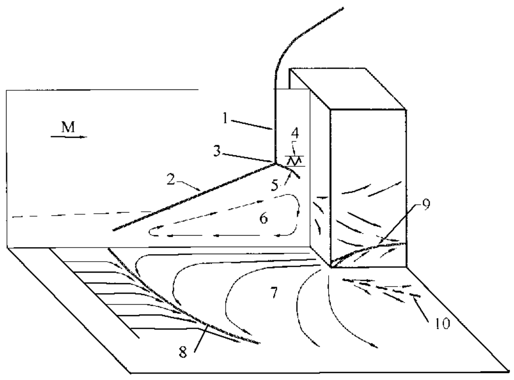


| | |
|---|---|
| 1 Bow shock | 2 Separated shock |
| 3 Triple point | 4 Oblique shock |
| 5 Tiny shock | 6 Separated region |
| 7 Surface friction line | 8 Separated line |
| 9 Separated line | 10 Reattached line |

Fig. 2. Separated flowfield pattern.

## *3.2 Shock Wave System in the Flowfield*

The schlieren photos show the shock wave system in the interactive regions in Fig. 3.

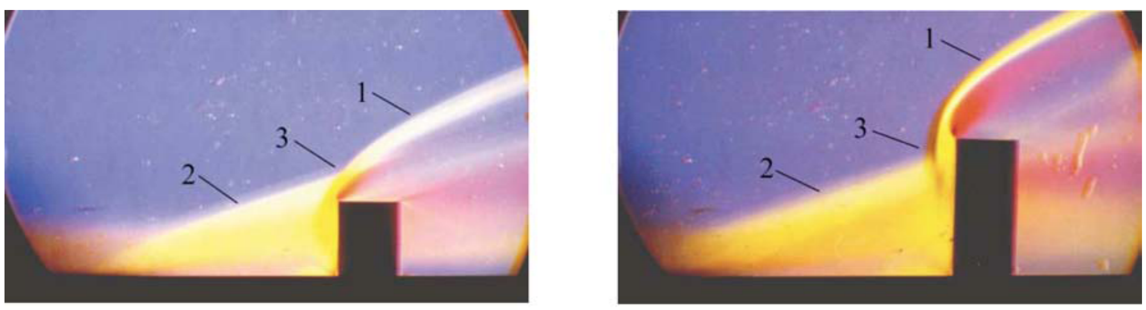


(a) $H/D=1.2$ (b) $H/D=2.2$

Fig. 3. Schlieren photos for $H/D=1.2$ and 2.2.

For two different parameters *H*/*D*, the separated shock and main shock crossed each other at different positions. For the case $H/D=1.2$, the cross point is over the top of the cylinder (see Fig. 3(a)). For case $H/D\geq 2.2$, the point 3 moves to the front of the leading edge of the cylinder. The complicated shock waves impinge to the cylinder leading edge (shown in Fig. 3(b)), then the peak loads (peak pressure and peak heat flux) impact to the cylinder surface.

The shock "1" can be evaluated by 2D inviscid flow theory, but it is difficult to predict for other shocks.

The photos indicate that the separated region expands to upstream with *H*/*D* increased.

## *3.3 The Oil Flow Pattern on the Surface*

In Fig. 4, the oil flow patterns show the skin frictions (made by mixed oil with $TiO_2$ powder)(Li et al., 1996). The separated boundary was formed by converged skin friction lines in Fig. 2, and the reattached line was a virtual line, from which many skin friction lines diverged. The distance *S* between leading edge of cylinder and separated boundary was measured for different parameter of *H*/*D*.

(a)

(b)

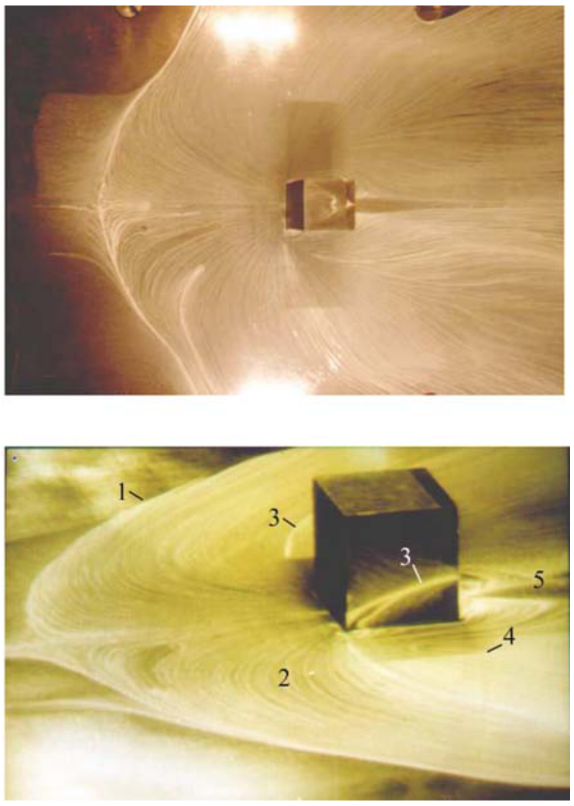


1 separated line
2 skin friction lines in separated region
3 second separated line
4 reattached line
5 weak

Fig. 4. (a) Oil flow pattern from top view. (b) Oil flow pattern from side view.

In Figs. 4(a) and 4(b), the top view and side view of the oil flow patterns for $H/D$=1.6 and $H/D$=1.2 are given respectively. In Fig. 4(b), the separated lines on the side surface of the cylinder, can clearly be seen. It expresses that the second or third separated vortex was born close to the corner.

### *3.4 Static Pressure Distributions*

The static pressure $P$ was measured by pressure transducers through the holes on the model surface. The freestream static pressure $P_s$ was measured by a pitot tube and also by transducers on the undisturbed flat plate.

Figure 5(a) shows the $P/P_s$ distributions along center line on the flat plate, and $X$ is normalized by $D$ ($D/d$ about 1.14). The parameter $H/D$ is from 0.2 to 2.2, corresponding to the peak pressure value from 2.6 to 12.5, and

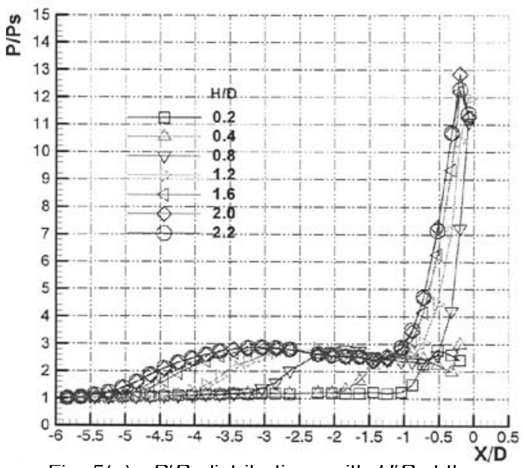


Fig. 5(a). $P/P_s$ distributions with $H/D$ at the symmetric line on the flat plate.

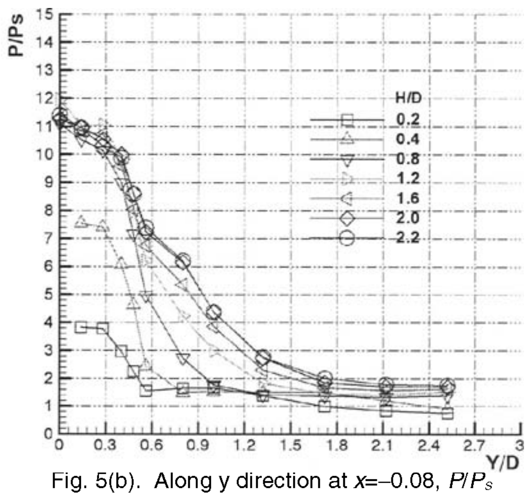


Fig. 5(b). Along y direction at $x$=–0.08, $P/P_s$ distributions with $H/D$ on the flat plate.

the influence region expands to $X/D$>5.0 in front of the leading edge of the cylinder. In this region, all of $DP$ (=$P - P_s$) are positive.

At $X/D$=−0.08 in Y/D direction, Figure 5(b) shows that the $P/P_s$ decreased from 11.5 to 1.0 for various $H/D$.

Figures 6(a) and 6(b) show the $P/P_s$ pressure contour on the flat plate for $H/D$=1.2 and 2.0. It is easy to observe the influence region in both sides of the cylinder. The pressure level is marked with different color.

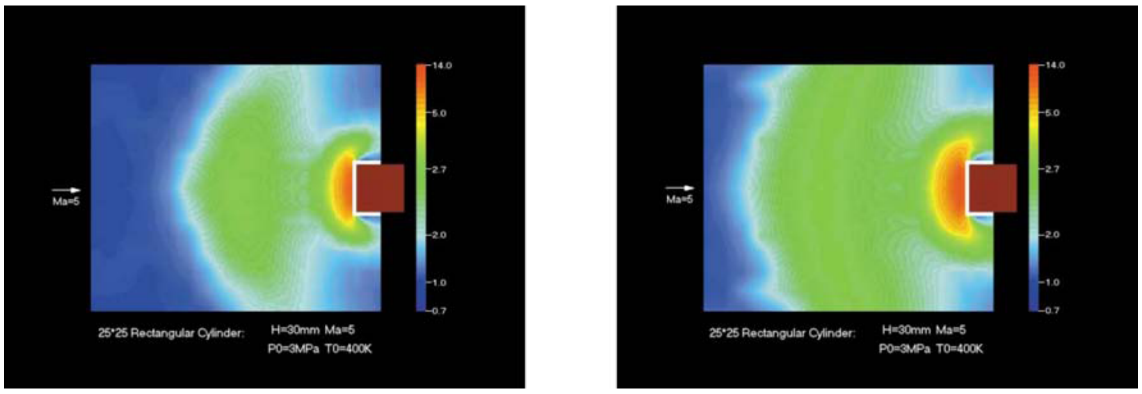


(a) $H/D$ =1.2 (b) $H/D$ =2.0

Fig. 6. $P/P_s$ pressure contour on the flat plate for $H/D$ =1.2 and 2.0.

At the symmetric line of the cylinder leading edge, the $P/P_s$ distributions along $Z/D$ are shown in Fig. 7. The peak pressure value is about 60, corresponding to the location which is behind the triple point of the shock wave system. It is almost 1.8 times over the $P/P_s$ value behind the 2D bow shock at "1" position (marked in Figs. 2 and 3).

The peak pressure is induced by crossed shock waves, and it is of importance in predicting the positions of the peak heating flux.

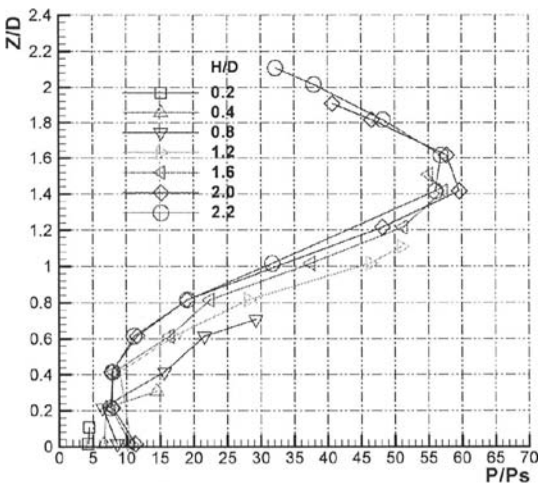


Fig. 7. $P/P_s$ distributions with $H/D$ on the rectangular cylinder windward along the symmetric line.

All of the figures (3, 4, 5, 6 and 7) and Table 1 indicate that for $H/D$ more than 2.0, the flowfield features including peak pressure level and separation region are independent of $H/D$, for $H/D$ less than 2.0, all of these features would vary with $H/D$.

We found that when the flow passes by the rectangular corner, it should be expanded and the pressure $P$ on the flat plate is reduce to less than $P_s$ somewhere. The $P/P_s$ distributions along the $X/D$ at $Y/D$=−0.56 (very close to the side wall of the rectangular cylinder on the flat plate) are listed in Table 1 corresponding to various $H/D$.

The regions of $P/P_s$ less than 1.0 are shown in Table 1, it is very different from the flow passing by the circular cylinder. Actually, we cannot find the same region where $P/P_s$ is less than 1.0 around the circular cylinder.

Table 1. At *y/D* =–0.56, $P/P_S$ varied with *H/D* and *X/D*.

| $H/D$ / $P/P_S$ / $X/D$ | 0.2 | 0.4 | 0.8 | 1.2 | 1.6 | 2.0 | 2.2 |
|---|---|---|---|---|---|---|---|
| 0 | 1.56 | 2.24 | 3.18 | 3.56 | 3.86 | 4.31 | 4.71 |
| 0.08 | 1.11 | 1.07 | 1.05 | 1.06 | 1.14 | 1.29 | 1.96 |
| 0.2 | 0.93 | 0.86 | 0.93 | 0.95 | 1.01 | 1.07 | 1.28 |
| 0.34 | 0.99 | 0.89 | 1.06 | 1.27 | 1.42 | 1.55 | 1.6 |
| 0.48 | 1.06 | 0.89 | 1.03 | 1.31 | 1.63 | 1.78 | 1.7 |

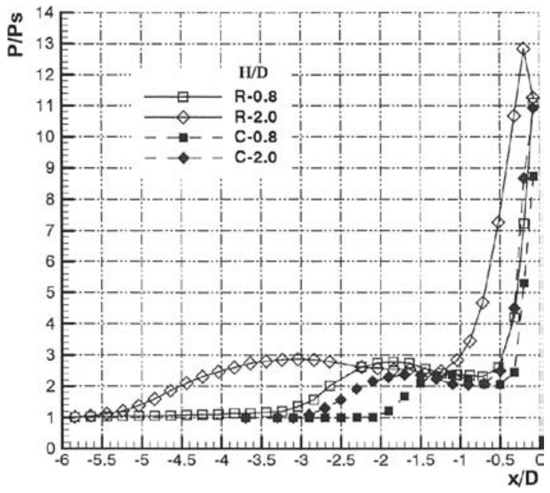


Fig. 8. A comparison for rectangular and circular cylinder on $P/P_S$ distributions along center line at the flat plate (*H/D* =0.8, 2.0).

The comparison of $P/P_s$ on rectangular and circular cylinders at the same test conditions for *H/D*=0.8 and 2.0 is shown in Fig. 8. It indicates that the influence of the cylinder radius on the interactive flowfield, from definite to infinite radius also including the results (Li et al., 1998 and 2000). The influence region for rectangular cylinder is wider than other cases. The largest influence region is corresponding to the case of *H/D* over 2. This result may work as a guide for many engineering problems. The detailed effects of Mach number and parameter *D*/*d* on interactive flowfield features are still open for further investigation.

## 4. Conclusions

A study on shock wave/turbulent boundary layer interaction induced by a set of rectangular cylinder was performed experimentally at Mach number 5.0, Reynolds number per meter of $5.3\times10^7$/m$^{-1}$. The rectangular cylinder is the limit case of circular cylinder, its radius of the cylinder at the leading edge tends to infinity. For various cylinder geometry with the same parameters *H/D*, *d*/*D*, the influence range of separated region and the pressure distribution corresponding to the rectangular cylinder is the largest.

The experimental results obtained by schlieren photographs, oil flow patterns and measured static pressure distributions show that

(1) If the parameter *H/D* is more than 2.0, the flowfield features are independent of *H/D*;

(2) If the parameter *H/D* is less than 1.5, the flowfield features depend on *H/D* strongly;

(3) Between the above cases, the flowfield will change slowly with varying parameter *H/D*;

(4) In the interactive region, somewhere very close to the front shoulder corner on the flat plate, low pressure levels ($P < P_S$) were found by the measured static pressure. Furthermore the second separated line from the corner was discovered. We did not find these results for flow over circular cylinder cases.

### Acknowledgments

This work was partly supported by National Natural Science Foundation of China. The authors greatly acknowledge this source of support.

### References

Chen, Y. K., Li, S. X. and Shi, Y. D., A Classification Study of Interaction between Cylinder and Turbulent Boundary Layer in Hypersonic Flow, 47th International Astro-nautical Congress (Beijing, China), (1996), ST-96-W.2.08.

Dolling, D. S. and Bogdonoff, S. M., Scaling of Interactions of Cylinders with Supersonic Turbulent Boundary Layer, AIAA 81-4110, (1981).

Dollong, D. D. and Smith, D. R., Separation Shock in Mach 5 Turbulent Interactions Induced by Cylinders, AIAA Journal, 27-12 (1989).

Holden, M. S., Shock Wave / Boundary Layer Interaction in Hypersonic Flow, AIAA-72-74, (1972).

Korkegi, R. H., Survey of Viscous Interactions Associated with High Mach Number Flight, AIAA Journal, 9-5 (1972-5), 771-784.

Li, S. X. and Chen, Y. K., A Comparison of Separated Flow Patterns Induced by Rectangular and Circular Cylinders, 8th International Symposium on Flow Visualization (Sorrento), (Sep., 1998) , Editors: G. M. Carlomagno and I. Grant, CD-ROM Proceedings ISBN 0 953399109.

Li, S. X., Chen, Y. K. and Ni, Z. Y., Investigation of the Separated Flow over Rectangular Obstacles, ACTA AERODYNAMICA SINICA, Vol.18, (2000-5).

Li, S. X., Chen, Y. K. and Ni, Z.Y., Pressure Measurement and Flow Visualization on Hypersonic Flow over Rectangular Cylinders, Sixth Triennial International Symposium on Fluid Control Measurement and Visualization (Sherbrooke, Canada), (2000-8), Editor: Andre Laneville, Proceedings ISBN 2-7622-0126-8.

Li, S. X., Shi, Y. D. and Chen, Y. K., The Effects of Short Protuberances on Interaction Flowfield at Hypersonic Speed, AIAA 95-1829, (1995).

Li, S. X., Shi, Y. D. and Chen, Y. K., Oil Flow Visualization by Real Time Injective Technique, Proceeding of the Fourth Asian Symposium on Visualization (Beijing, China), (1996), 115-119.

Miller, W. H., Pressure Distribution on Single and Tandem Cylinders Mounted on a Flat Plate in Mach 5.0 Flow, AD 634282, (1966).

Sedney, R., A Survey of the Effects of Small Protuberences on Boundary Layers, AIAA Journal, 11-6, (1973).

Settles, G. S. and Dolling, D. S., Swept Shock Wave / Boundary Layer Interaction, Tactical Missile Aerodynamics, Editors: M. J. Hemsh and J. N. Nielson, (1986).

### Author Profile

Suxun Li: She graduated from Beijing Institute of Aeronautics in 1959. Then she worked in department of Aircraft Engineering, Northwest Polytechnic University from 1959 to 1974. Since 1974 she has been working in Beijing Institute of Aerodynamics (BIA), currently as a professor in BIA and Beijing University of Aeronautics and Astronautics. She is a council member and a director of hypersonic flow committee of Chinese Aerodynamics Research Society. Her research interests are also in numerical simulation, complex flow (separated flow, vortex flow) experimental technique and flow visualization technique. She was a faculty visiting professor in Mechanical Engineering of California State University (Long Beach) from 1985 to 1987.

Yongkang Chen: He received his bachelor (1992) in Engineering Mechanics from Beijing University of Aeronautics and Astronautics (BUAA) and his master (1995) in Aerodynamics from BIA. Then he worked in BIA from 1995 to 1998. He is currently pursuing a Ph.D. at Purdue University in America from 1998 to now. His research interests are in experimental aerodynamics and engineering design problems.

Zhaoyong Ni: He received his bachelor (1992) in Engineering Mechanics from BUAA and his master (1995) in Aerodynamics from BIA. Then he worked in BIA from 1995 to 2000. He begins to pursue a Ph.D. at BIA under the direction of Suxun Li in 2000. His interests are in computational fluid mechanics and experimental techniques.